Time-varying linear and nonlinear parametric model for Granger causality analysis

Yang Li,[1,2,*] Hua-Liang Wei,[2] Steve A. Billings,[2] and Xiao-Feng Liao[1]

[1]*Department of Computer Science and Engineering, Chongqing University, China*
[2]*Department of Automatic Control and Systems Engineering, The University of Sheffield, Mapping Street, S1 3JD Sheffield, United Kingdom*

Statistical measures such as coherence, mutual information, or correlation are usually applied to evaluate the interactions between two or more signals. However, these methods cannot distinguish directions of flow between two signals. The capability to detect causalities is highly desirable for understanding the cooperative nature of complex systems. The main objective of this work is to present a linear and nonlinear time-varying parametric modeling and identification approach that can be used to detect Granger causality, which may change with time and may not be detected by traditional methods. A numerical example, in which the exact causal influences relationships, is presented to illustrate the performance of the method for time-varying Granger causality detection. The approach is applied to EEG signals to track and detect hidden potential causalities. One advantage of the proposed model, compared with traditional Granger causality, is that the results are easier to interpret and yield additional insights into the transient directed dynamical Granger causality interactions.

PACS number(s): 87.10.−e, 05.45.Tp, 05.10.−a, 87.19.le

I. INTRODUCTION

In cognitive neuroscience, as in many other science and engineering research fields, the investigation of EEG data is usually carried out by some measures of correlation, coherence, and mutual information [1]. These measures, however, provide no insight into the directionality of information flow. A question of great interest is whether there exist causal relations among a set of measured variables. Several recent works based on vector autoregressive (VAR) models have begun to consider this problem [2]. Causal relations between different components of a multidimensional signal can be analyzed in the context of multivariate autoregressive modeling. The most popular approach to deal with the causal relations is the Granger causality [3]. The major approach to causality examines whether the prediction of one series could be improved by incorporating information from the other, as discussed by Granger. In particular, if the prediction error of the signal X is reduced by including measurements from the signal Y in the regressor model, then the signal Y is said to have a causal influence on the signal X. Granger causality was originally investigated for linear systems. Recently, this concept was extended to nonlinear cases. The application of Granger causality to neuroscience data has been applied to functional magnetic resonance imaging (fMRI) [4], Electroencephalography (EEG) [5,6], and Magnetoencephalography (MEG) experiments [7].

Linear time-varying causality was previously investigated on scalp EEG [5]. Hesse *et al.* [5] studied the linear recursive time-variant estimation of the Granger causality based on the adaptive recursive fit of a VAR model with time-varying parameters by means of the recursive least-squares (RLS) algorithm, where the assumption of stationarity of the signals can be removed. Recently, the Granger causality definition was extended to nonlinear bivariate time series [8,9]. Gourevitch *et al.* [10] have evaluated the measures of Granger causality on some linear and nonlinear models, and they have also investigated some of the properties and drawbacks for linear and nonlinear Granger causality.

All traditional Granger causality detection methods are based on the time-invariant linear autoregressive with exogenous inputs (ARX) models or time-invariant nonlinear models. It follows that standard linear VAR models may not always be able to capture the dynamic behavior of many nonstationary time series. To the best of our knowledge, results on time-varying nonlinear Granger causality analysis have seldom been reported in the literature. In this paper, we will introduce a nonlinear method that can be used to detect and track nonlinear dynamical Granger causalities. To illustrate the performance of the method, two examples are presented: one for artificial data where the exact causal effect feature is known, and another for real EEG data where the hidden causality feature is revealed by the proposed method.

II. METHOD

A. Time-varying linear Granger causality

Granger causality is a fundamental tool for the description of causal interactions of two time series. We detail the bivariate case of the Granger causality in this paper.

1. Time-invariant Granger causality

Let X and Y be two signals whose time observations are denoted $x(t)$ and $y(t)$, with $t = 1,2,\ldots,N$. In order to show the improvement of the prediction of one signal by taking into consideration the past of the second signal, the univariate autoregressive (AR) and bivariate ARX models are fitted to the signals, respectively. If the temporal dynamics of $x(t)$ and $y(t)$ are suitably represented by a time-varying univariate AR model of order p, we can obtain

$$x(t) = \sum_{i=1}^{p} a_{1,i} x(t-i) + u_1(t), \qquad (1)$$

$$y(t) = \sum_{i=1}^{p} b_{1,i} y(t-i) + u_2(t), \qquad (2)$$

*coq08yl@gmail.com

where the prediction error for a signal depends only on the past of its own signal. The time- varying bivariate ARX(p,q) model is represented by

$$x(t) = \sum_{i=1}^{p} a_{2,i} x(t-i) + \sum_{k=1}^{q} c_{2,k} y(t-k) + v_1(t), \quad (3)$$

$$y(t) = \sum_{i=1}^{p} b_{2,i} y(t-i) + \sum_{k=1}^{q} d_{2,k} x(t-k) + v_2(t), \quad (4)$$

where the prediction errors v_1 and v_2 depend on the past of the signal itself and additionally on the past of the second signal. The coefficients in the model (1)–(4) are generally estimated by solving Yule-Walker equations [11], which require the stationarity of the signals and result in the time-invariant VAR model analyzed over the course of time.

Let us begin with the bivariate case of causality $X \rightarrow Y$. The reciprocal case is similar. The accuracy of the prediction in model (1) and (2) may be evaluated by the unbiased variance of the prediction errors $\sum_{y|y^-}$, where y^- symbolizes y past

$$\sum\nolimits_{y|y^-} = \frac{1}{N-p} \sum_{t=1}^{N} u_2^2(t) = \frac{R_{y|y^-}^{\text{RSS}}}{N-p} = \text{var}(u_2), \quad (5)$$

where $R_{y|y^-}^{\text{RSS}}$ is the residual sum of squares (RSS) in the model (2). For the bivariate model (3) and (4), we can obtain

$$\sum\nolimits_{y|y^-,x^-} = \frac{1}{N-p-q} \sum_{t=1}^{N} v_2^2(t) = \frac{R_{y|y^-,x^-}^{\text{RSS}}}{N-p-q} = \text{var}(v_2). \quad (6)$$

If the signal X causes the signal Y in the Granger sense, the variance of the prediction error $\sum_{y|y^-,x^-}$ must be smaller than the prediction error $\sum_{y|y^-}$. The linear Granger causality (LGC) $X \rightarrow Y$ is then defined by [10]

$$C_{x \rightarrow y}^{\text{LGC}} = \ln \frac{\sum_{y|y^-}}{\sum_{y|y^-,x^-}}. \quad (7)$$

Correspondingly, the LGC of $Y \rightarrow X$ is evaluated by

$$C_{y \rightarrow x}^{\text{LGC}} = \ln \frac{\sum_{x|x^-}}{\sum_{x|x^-,y^-}}. \quad (8)$$

Generally, the most important property of the Granger causality is the positivity, when a signal X causes a second signal Y. Equations (7) and (8) represent a simple measure for the strength of directional interaction.

2. Time-varying causality measure

The time-varying fit of a VAR model is required to detect the transient directed interactions. Ding *et al*. [12] investigated a VAR model fitting algorithm to obtain the time-varying Granger causality, which requires us to assume that the signals to be studied are stationary within a short-time window, and the changes from one window to another are smooth. There is a limitation in the effectiveness for this approach. First, if the processes are varying rapidly, a process assumed to be stationary may be too small to allow for sufficient accuracy in

the estimation of the relevant parameters over the window. Second, this approach would not easily accommodate the step changes with the analysis intervals. Third, this solution imposes an incorrect model on the observal data, that is, piecewise stationary. Therefore, an adaptive recursive fit of a VAR model with time-dependent parameters by means of some adaptive filtering procedures such as recursive-least-squares (RLS), least-mean-squares (LMS), and Kalman filtering algorithms is proposed to capture the transient Granger causality. The time-varing VAR model fitting can yield time-varying autoregressive parameters. Consequently, by contrast with the model (1)–(4), the time-varying VAR models are represented by

$$x(t) = \sum_{i=1}^{p} a_{1,i}(t) x(t-i) + u_1(t), \quad (9)$$

$$y(t) = \sum_{i=1}^{p} b_{1,i}(t) y(t-i) + u_2(t), \quad (10)$$

and

$$x(t) = \sum_{i=1}^{p} a_{2,i}(t) x(t-i) + \sum_{k=1}^{q} c_{2,k}(t) y(t-k) + v_1(t), \quad (11)$$

$$y(t) = \sum_{i=1}^{p} b_{2,i}(t) y(t-i) + \sum_{k=1}^{q} d_{2,k}(t) x(t-k) + v_2(t). \quad (12)$$

The time-varying fit of VAR models yields the time-varying variance of the prediction error. A general recursive variance computational formula can be defined by

$$\sigma^2(t+1) = (1-c)\sigma^2(t) + c\Delta^2(t), \quad (13)$$

where the constant lies at $0 < c < 1$, and $\Delta(t)$ is one of $u_1(t)$, $u_2(t)$, $v_1(t)$, and $v_2(t)$, which represent the time-varying variances of the correspondent prediction errors $\sum_{x|x^-}(t)$, $\sum_{y|y^-}(t)$, $\sum_{x|x^-,y^-}(t)$, and $\sum_{y|y^-,x^-}(t)$.

Therefore, the representation of time-varying LGC is then evaluated by [10]

$$C_{x \rightarrow y}^{\text{LGC}}(t) = \ln \frac{\sum_{y|y^-}(t)}{\sum_{y|y^-,x^-}(t)}, \quad (14)$$

$$C_{y \rightarrow x}^{\text{LGC}}(t) = \ln \frac{\sum_{x|x^-}(t)}{\sum_{x|x^-,y^-}(t)}. \quad (15)$$

The calculation of the time-varying Granger causalities in Eqs. (14) and (15) is analogous to Eqs. (7) and (8). The time-varying strength of interaction may be quantified by the maximum at each time point from Eqs. (14) and (15).

B. Time-varying nonlinear Granger causality

In this subsection, our main purpose is to find the general VAR model suitable to evaluate Granger causality, thus extending the radial basis functions (RBFs) model results discussed in Ref. [9].

1. NARX model

The identification problem of a nonlinear dynamical system is based on the observed input-output data $\{x(t),y(t)\}_{t=1}^N$, where $x(t)$ and $y(t)$ are the observations of the system input and output, respectively [13]. This study considers a class of discrete stochastic nonlinear systems which can be represented by the following nonlinear autoregressive with exogenous inputs (NARX) structure [14–17]:

$$y(t) = f(y(t-1),\ldots,y(t-n_y),x(t-1),\ldots, \\ \times\, x(t-n_x),\theta) + e(t),\qquad(16)$$

where $f(\cdot)$ is the unknown system mapping; $x(t)$, $y(t)$, and $e(t)$ are the system input and output variables and the prediction error, respectively; n_x and n_y are the maximum input and output lags, respectively; and the observation noise $e(t)$ is an uncorrelated zero mean noise sequence providing that the function $f(\cdot)$ gives a sufficient description of the system. If the function $f(\cdot)$ is specified as a polynomial function, model (16) can then be represented by

$$y(t) = f[\varphi(t)] + e(t),\qquad(17)$$

where $\varphi(t) = [y(t-1),\ldots,y(t-n_y),x(t-1),\ldots, x(t-n_x)]^T$ is the process regressor vector. The polynomial NARX model is a special case of the polynomial NARMAX model [18,19]. The nonlinear mapping $f(\cdot)$ of Eq. (17) can be constructed using a class of local or global basis functions including RBFs, kernel functions, neural networks, wavelets, and different types of polynomials [18–26].

The polynomial bivariate model representation of NARX is represented by a compact matrix,

$$y(t) = \sum_{m=1}^M \alpha_m \Phi_m(t) + e_2(t),\qquad(18)$$

where $\Phi_m(t) = \Phi_m[\varphi(t)]$ are model terms generated from the regressor vector $\varphi(t) = [y(t-1),\ldots,y(t-n_y),x(t-1),\ldots,x(t-n_x)]^T$, α_m are unknown parameters, and M is the total number of potential model terms. Note that the candidate model terms $\Phi_m(t)$ are of the form $x_1^{i_1}(t),\ldots,x_d^{i_d}$, where d refers to the nonlinear degree of the NARX model (18), $x_k^{i_k}(t) \in \{y(t-1),\ldots,y(t-n_y),x(t-1),\ldots,x(t-n_x)\}$, for $k=1,\ldots,d$, $0 \leqslant i_k \leqslant d$, and $0 \leqslant i_1 + \cdots + i_d \leqslant d$. The maximum lag of the polynomial model (17) is determined by n_y and n_x. The number of possible terms could be very large, and the number of polynomial terms (number of parameters) is $n_p = \frac{(n_y+n_x+d)!}{(n_y+n_x)!\,d!}$, for example, if $n_y = 5$, $n_x = 5$ and $d = 4$, $n_p = 1001$. As to the nonlinear degree determination issue, the experience of practical modeling and identification has shown that, if the lower degree of the nonlinear degree, for example $d = 1$ for maximum lag n_y and n_x, is insufficient to represent the original system, then a series of polynomial models with a higher degree should be fitted to give a sufficient description of the data set. In particular, if the nonlinear degree d of the NARX model (18) is reduced to 1, the NARX model will be simplified to the linear ARX model described in Eqs. (1) and (2).

The corresponding polynomial univariate NAR model can also be expressed by

$$y(t) = \sum_{m=1}^{M_0} \beta_m \Psi_m(t) + e_1(t),\qquad(19)$$

where $\Psi_m(t) = \Psi_m[\varphi^*(t)]$ are model terms generated from the regressor vector $\varphi^*(t) = [y(t-1),\ldots,y(t-n_y)]^T$, β_m are unknown parameters, and M_0 is the total number of potential model terms.

The prediction error of the bivariate NARX model (18) (we assume $M \gg n_y + n_x$) can be expressed by

$$\sum\nolimits_{y|y^-,x^-} = \frac{1}{M}\sum_{m=1}^M [y(t) - \alpha_m \Phi_m(t)]^2.\qquad(20)$$

We can also consider the univariate NAR model (19) and obtain the corresponding prediction error

$$\sum\nolimits_{y|y^-} = \frac{1}{M_0}\sum_{m=1}^{M_0} [y(t) - \beta_m \Psi_m(t)]^2.\qquad(21)$$

If the prediction of y improves by incorporating the past value of x, i.e., $\sum_{y|y^-,x^-}$ is smaller than $\sum_{y|y^-}$, then x is said to have a causal influence on y.

Modeling experience has shown that in most cases, the initial full regression Eq. (18) might be highly redundant. Some of the regressors or model terms can be removed from the initial regression equation without any effect on the predictive capability of the model, and this elimination of the redundant regressors usually improves the model performance [27]. The ordinary least-squares algorithm may fail to produce reliable parametric estimate results for such ill-posed problems. For most nonlinear dynamical system identification problems, only a relatively small number of model terms are commonly required in the regression model. Thus an efficient model term selection algorithm is highly desirable to detect and select the most significant regressors.

2. Model structure identification

The well-known orthogonal-least-squares (OLS) type of algorithms [16,17,19,20,23,24,27–30] have proven to be very effective to solve multiple dynamical regression problems, where a great number of candidate model terms or regressors that may be highly correlated include the regressor model. In the present study, the OLS algorithm discussed in Ref. [23] is applied to deal with the regression model (18). This involves a model refinement procedure including the selection of significant regressor or model terms.

3. Time-varying nonlinear model and parameter estimation

The time-varying (TV) VAR model fitting for the bivariate NARX and the univariate NAR model yields time-varying autoregressive parameters. Consequently, after a model refinement procedure, Eqs. (18) and (19) are modified as

follows:

$$y(t) = \sum_{m=1}^{M^*} \alpha_m^*(t) \Phi_m^*(t) + e_2^*(t) \quad \text{for the TVNARX model,}$$

(22)

$$y(t) = \sum_{m=1}^{M_0^*} \beta_m^*(t) \Psi_m^*(t) + e_1^*(t) \quad \text{for the TVNAR model,}$$

(23)

where M^*, M_0^* are the total number of selections of significant regressors for the bivariate NARX and the univariate NAR model, respectively, $(M^*, M_0^* \leqslant M)$, α^* and β^* are time-varying parameters, Φ^* and Ψ^* are new model terms selected from the regressors vector $\varphi(t)$ and $\varphi(t)^*$, and e_2^* and e_1^* are the time-varying model prediction error, respectively. An online RLS algorithm is then applied to estimate the time-varying model parameters. But other online methods, for example a Kalman filtering algorithm, can also be employed to estimate the unknown time-varying parameters. While the tracking ability of RLS is achieved by performing a forgetting factor operation on the information matrix, the tracking capability of Kalman filtering is obtained by adding a non-negative definite matrix to the covariance matrix. The main reason for employing RLS in the present study is mainly its simple calculation and good convergence properties.

4. Time-varying nonlinear Granger causality measure

Similar to the definition of linear Granger causality, let us begin with the bivariate case of causality $x \rightarrow y$. For model (18) and (19), the unbiased variance may be evaluated by the variance of prediction error described in Eqs. (20) and (21). The time-varying estimation of the VAR model (22) and (23) leads to time-varying prediction error. A general time-varying recursive variance computation is given in Eq. (13). If x causes y in the Granger causality sense, $\sum_{y|y^-,x^-}$ must then be smaller than $\sum_{y|y^-}$. Therefore, for the time-varying model (22) and (23), the calculation of time-varying nonlinear Granger causality can be evaluated by

$$C_{x \rightarrow y}^{\text{NGC}}(t) = \ln \frac{\sum_{y|y^-}(t)}{\sum_{y|y^-,x^-}(t)},$$

(24)

where $\sum_{y|y^-,x^-}(t)$ and $\sum_{y|y^-}(t)$ are the time-varying variance of the corresponding prediction error for the model (22) and (23), respectively. Exchanging the two time series, one may analogously study the time-varying nonlinear Granger causality influence of y on x. It is worth stressing that, within the definition of causality, for the time-series data the directed flow of time plays a key role in making inferences, depending on the direction. Note that Granger causality was initially formulated for linear models, which may not be suitable for causality evaluation for nonlinear time series. Ancona *et al.* [8] and Marinazzo *et al.* [9] extended the definition of Granger causality to nonlinear bivariate time series, and proposed that any prediction scheme providing a nonlinear extension of Granger causality should satisfy the following property: if the time series $\{x(t)\}_{t=1}^{N}$ is statistically independent of $\{y(t)\}_{t=1}^{N}$, then $\sum_{y|y^-,x^-} = \sum_{y|y^-}$; if $\{y\}_{t=1}^{N}$ is statistically independent $\{x(t)\}_{t=1}^{N}$, then $\sum_{x|x^-,y^-} = \sum_{x|x^-}$. The property holds at least for $M \rightarrow \infty$. The polynomial NARX structure model is the largest class of nonlinear parametric models suitable to evaluate causality. Ancona *et al.* [8] introduced the nonlinear parametric model to evaluate the causality based on a class of RBF model as a special case of the polynomial NARX structure model. It should also be noted that time-varying linear Granger causality is a special case of the time-varying NARX model to evaluate the Granger causality where the nonlinear degree d in the NARX model is equal to 1.

C. Choice of the model order

As to the model order determination issue, this can be solved by using some model order determination criterion such as the Akaike information criterion (AIC), the Bayesian information criterion (BIC) [31], the minimum description length (MDL) principle [32], the generalized cross-validation (GCV) criterion [23,30], or the visual fitting quality of the model [33].

III. SIMULATION EXAMPLE

In this section, we consider a simulation example that shows the ability of the time-varying Granger causality to react to changes in the directed influences between two signals. Consider the following time-varying ARX (2, 2) model:

$$y(t) = b_{2,1}(t) y(t-1) + b_{2,2}(t) y(t-2) + d_{2,1}(t) x(t-1) + d_{2,2}(t) x(t-2) + v_2(t),$$
$$x(t) = a_{2,1}(t) x(t-1) + a_{2,2}(t) x(t-2) + c_{2,1}(t) y(t-1) + c_{2,2}(t) y(t-2) + v_1(t),$$

(25)

where

$$a_{2,1}(t) = \begin{cases} -0.6, & 1 \leqslant t < 400, \\ 0.3, & 400 \leqslant t \leqslant 1000, \end{cases} \qquad b_{2,1}(t) = \begin{cases} 0.3, & 1 \leqslant t < 400, \\ -0.6, & 400 \leqslant t \leqslant 1000, \end{cases}$$

$$a_{2,2}(t) = 0.1, \ 1 \leqslant t \leqslant 1000, \qquad b_{2,2}(t) = 0.1, \ 1 \leqslant t \leqslant 1000,$$

$$c_{2,1}(t) = \begin{cases} 0.2, & 1 \leqslant t \leqslant 300, \\ 0, & 300 < t \leqslant 1000, \end{cases} \qquad d_{2,1}(t) = \begin{cases} 0, & 1 \leqslant t < 700, \\ 0.2, & 700 \leqslant t \leqslant 1000, \end{cases}$$

$$c_{2,2}(t) = \begin{cases} 0.1, & 1 \leqslant t \leqslant 300, \\ 0, & 300 < t \leqslant 1000, \end{cases} \qquad d_{2,2}(t) = \begin{cases} 0, & 1 \leqslant t < 700, \\ 0.1, & 700 \leqslant t \leqslant 1000, \end{cases}$$

(26)

and v_1, v_2 are Gaussian white noise processes with zero means and variances

$$\text{var}(v_1) = \begin{cases} 0.9, & 1 \leqslant t < 600, \\ 2.0, & 600 \leqslant t \leqslant 1000, \end{cases} \quad \text{var}(v_2) = \begin{cases} 2.0, & 1 \leqslant t < 600, \\ 0.9, & 600 \leqslant t \leqslant 1000, \end{cases} \tag{27}$$

respectively. From the construction of the model, we can see, for the first 300 sample points, that signal y causes signal x and, beginning with the sample point 700, signal x causes signal y. From sample point 301 up to sample point 699, there is no dependence between the two signals x and y. The results of time-varying Granger causalities are shown in Fig. 1.

From the Fig. 1, the time-limited influence of $x \to y$ beginning with the sample index point 700 is detected by the positivity of $C_{x \to y}^{\text{LGC}}(t)$ [thick blue (upper) curve]. The time-limited influence of $y \to x$ for the first 300 sample index points is identified by the positivity of $C_{y \to x}^{\text{LGC}}(t)$ [black (lower) curve]. Obviously both Granger causalities are nearly zero within the time interval ($300 < t < 700$) without any dependence between the two signal components. Moreover, time-varying Granger causalities vary around the estimation of the corresponding time-invariant Granger causality (for example, thin black and blue curves) within the stationary time intervals $0 < t \leqslant 300$ and $700 \leqslant t \leqslant 1000$. In this simulation example, the time behavior of time-varying Granger causality demonstrates the ability to react to changes in directed dependencies between two signals.

IV. APPLICATION TO THE REAL EEG SIGNAL

A number of studies in the neuroscience literature have investigated examples of the issue of causal effects in neural data [5,7,9,12,33]. In this example, we analyze a data set consisting of an epileptic sample of scalp EEGs recorded by a clinician at the EEG Laboratory of Neurophysiology, Sheffield

Teaching Hospitals NHS Foundation Trust, Royal Hallamshire Hospital.

A. Data acquisition

Scalp EEG signals are synchronous discharges from cerebral neurons detected by electrodes attached to the scalp. The EEG signals analyzed here were recorded by the same 32-channel amplifier system. A NeuroScan Medical System (NeuroSoft Inc., Sterling, VA) with the international 10-20 electrode coupling system (Rechtschaffen & Kales 1968) was used. The sampling rate of the device was 250 Hz. An important issue in EEG data acquisition is the problem of the reference electrode. There are several ways to define a reference electrode in scalp EEG recordings, as described in Ref. [34]. However, not every type is suitable for the Granger causality analysis. For example, the "common average" reference involves all the channels as reference, and mixes signals from all of them. Generally, all operations where part of the signal from one channel appears in another channel will lead to a spurious connection. In the present case study, the "bipolar montage" reference was used. As an example, two bipolar montage channels "C3-T3" and "C4-T4" of EEG recorded from a patient with absence seizure epileptic discharge are investigated in this study, where channel "C3-T3" represents the voltage difference between C3 and T3, and channel "C4-T4" means the voltage difference between C4 and T4, respectively. The EEG signals between bipolar electrode channel "C3-T3" and channel "C4-T4" of 5000 data point pairs of one seizure, shown in Fig. 2, which are for a sort of epileptic seizure activity of a patient with a sampling rate of 250 Hz recording during 20 s, were obtained for time-varying Granger causality analysis. Based upon the advice of our

FIG. 1. (Color online) Time-varying Granger causalities $C_{x \to y}^{\text{LGC}}(t)$ [thick blue (upper) curve] and $C_{y \to x}^{\text{LGC}}(t)$ [black (lower) curve] from model (25) with time-varying parameters given in Eq. (26) are shown above. The thin blue and black step functions show that the corresponding estimated time-invariant Granger causalities are $C_{x \to y}^{\text{LGC}}$ and $C_{y \to x}^{\text{LGC}}$.
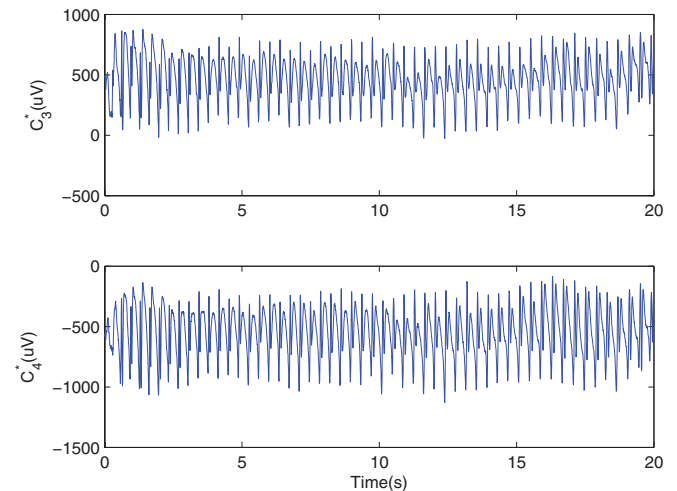
FIG. 2. (Color online) The EEG signals, for a sort of seizure activity of an epileptic patient, recorded during 20 s, with a sampling rate of 250 Hz, for both electrode channel C_3^* (above) and C_4^* (below).

clinician, we selected two channels "C3-T3" and "C4-T4" for the analysis of the causal influence. Here the bipolar channel "C3-T3" indicates the new electrode channel C_3^*, and the channel "C4-T4" denotes the new electrode channel C_4^*.

B. Time-varying nonlinear Granger causality for EEG signals

Generally, the most significant property of the Granger causality is its positivity in the case when a signal X causes a second signal Y. The time-varying NARX modeling approach under definition (23) is applied to real EEG signals to study the causal relationship between EEG signals C_3^* and C_4^* to demonstrate the behavior of the time-varying Granger causality. The NARX model with a nonlinear degree $d = 2$, maximum lags $n_y = 5$ and $n_x = 5$, and the total number of potential 66 regressor terms for different model orders was estimated using the OLS algorithm [23], and both the AIC and BIC criteria suggested that the model size can be chosen to be 6 from the total number of 66 regressor terms, with the bivariate case $C_3^* \to C_4^*$. Hence the time-varying NARX model and the univariate NAR model can be represented by, respectively,

$$
\begin{aligned}
y(t) = &\sum_{i=1}^{3} \theta_{1,i}(t) y(t-i) + \theta_{2,1}(t) x^2(t-1) \\
&+ \theta_{2,2}(t)\, x^2(t-2) + \theta_{2,5}(t) x^2(t-5) \\
&\text{for} \quad \text{TVNARX},
\end{aligned}
\tag{28}
$$

$$
y(t) = \sum_{i=1}^{3} \theta_i^*(t) y(t-i) \quad \text{for TVNAR}, \tag{29}
$$

Due to Eqs. (13), (28), and (29), the transient estimations of time-varying nonlinear Granger causality $C_{C_3^* \to C_4^*}^{\text{NGC}}(t)$ can be obtained. Similarly, exchanging the two EEG signals for bivariate $C_4^* \to C_3^*$, the time-varying Granger causality $C_{C_4^* \to C_3^*}^{\text{NGC}}(t)$ can also be obtained in both cases for $c = 0.005$.

Time-varying Granger causality in both directions was calculated for electrode pairs between C_3^* and C_4^*. A directed influence for a determined time interval is stated. Figure 3 illustrates a typical result for the electrode pair C_3^*/C_4^*. In Fig. 3, we depict the directed interactions $C_{C_3^* \to C_4^*}^{\text{NGC}}(t)$ [blue (upper) curve, measuring the influence of C_3^* on C_4^*] and $C_{C_4^* \to C_3^*}^{\text{NGC}}(t)$ [black (lower) curve, measuring the influence of C_4^* on C_3^*], as a function of sample time, for a sort of epileptic seizure activity of a patient. Figure 3 shows the result of the time-varying Granger causality to react to rapid changes in the directed influences between the channel C_3^* and C_4^*. From Fig. 3, two directed Granger causalities can be obviously observed. (i) For the chosen electrode pair C_3^*/C_4^*, the interaction is directed from the left central area (C_3^*) to the right central area (C_4^*) during all of the time interval course; the Granger causality $C_{C_3^* \to C_4^*}^{\text{NGC}}(t)$ is significantly larger in the whole time interval than $C_{C_4^* \to C_3^*}^{\text{NGC}}(t)$. Thus, a superior influence from C_3^* to C_4^* is present within this time interval. (ii) During the period from 10 to 12 s, the Granger causality influence between both C_4^* and C_3^* is weakened, especially around the time point 20 s, when the interaction is very small. It is worth noting that these causal relationships for the electrode pair C_3^*/C_4^* are not evident in terms of cross-correlation, which is
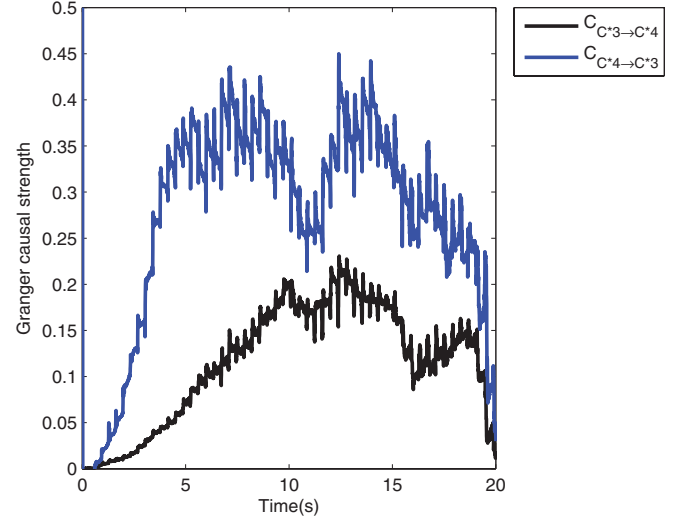
FIG. 3. (Color online) The time-varying nonlinear Granger causality $C_{C_3^* \to C_4^*}^{\text{NGC}}(t)$ [blue (upper) curve] and $C_{C_4^* \to C_3^*}^{\text{NGC}}(t)$ [black (lower) curve] are plotted vs the time courses for EEG signals shown in Fig. 2.

defined as

$$
c_1(\tau) = \frac{\sum_t [x(t-\tau) - \bar{x}][y(t) - \bar{y}]}{\sqrt{\sum_t [x(t) - \bar{x}]^2} \sqrt{\sum_t [y(t) - \bar{y}]^2}} \tag{30}
$$

and

$$
c_2(\tau) = \frac{\sum_t [x(t+\tau) - \bar{x}][y(t) - \bar{y}]}{\sqrt{\sum_t [x(t) - \bar{x}]^2} \sqrt{\sum_t [y(t) - \bar{y}]^2}}. \tag{31}
$$

$c_1(\tau)$ and $c_2(\tau)$ for some specific epileptic patient data are depicted in Fig. 4, which gives no interesting patterns that are possessed by the proposed time-varying NARX model. These properties, possessed by the proposed time-varying NARX model, cannot be obtained using any time-invariant parametric modeling framework for linear and nonlinear Granger causality of time series. It should also be stressed that, in the case of an optimal fit to the true autoregressive parameters
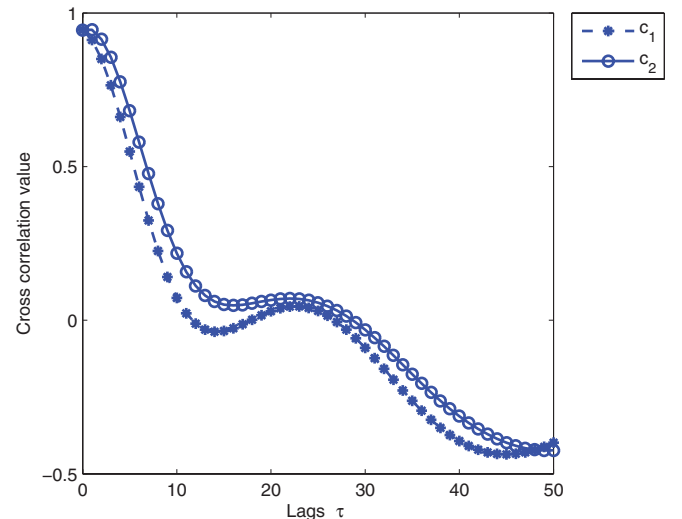
FIG. 4. (Color online) The cross correlations $c_1(\tau)$ and $c_2(\tau)$ are shown vs τ between EEG signals C_3^* and C_4^* given in Fig. 2.

of univariate and bivariate models, Granger causality is a non-negative value. Compared to the Granger causality analysis of the occurrence of a negative value due to the main reason of no optimal models in Ref. [5], our proposed approach in this study is effective. The results can help clinicians to interpret EEG signals.

V. CONCLUSIONS

In this paper, we have introduced the polynomial mathematical formalism and studied the question of how to evaluate time-varying linear and nonlinear Granger causal relations in neural systems. Demonstrations of the technique have been carried out on both simulated data, where the patterns of interactions are known, and on real EEG signals. This study mainly illuminates three essential aspects. First, the proposed method for time-varying linear estimation of Granger causality permits the detection of temporal causal interactions. Second, we have generalized the nonlinear parametric approach to Granger causality: the proposed model is not limited to being additive in variables from the two time series and can approximate any functions of these variables, including RBF, neural networks, multiresolution wavelet, and different types of polynomials such as the Chebyshev and Legendre types, still being suitable to evaluate causality. Finally, temporally directed interactions were detected successfully for electrophysiological

data of epileptic patients on the basis of transient Granger causality.

This study demonstrates the possibility of detecting and describing transient directed webs of interactions for the bivatiate case. In fact, the presented approach can be extended to the multivariate case and be suitable for the study of causal interactions between electrophysiological data of different sites of the scalp, occurring during the cognitive processes.

[1] R. Q. Quiroga, A. Kraskov, T. Kreuz, and P. Grassberger, Phys. Rev. E **65**, 041903 (2002).

[2] P. F. Verdes, Phys. Rev. E **72**, 026222 (2005).

[3] C. W. J. Granger, Econometrica **37**, 424 (1969).

[4] J. R. Sato, E. Amaro, D. Y. Takahashi, M. D. Felix, M. J. Brammer, and P. A. Morettin, NeuroImage **31**, 187 (2006).

[5] W. Hesse, E. Moller, M. Arnold, and B. Schack, J. Neurosci. Methods **124**, 27 (2003).

[6] K. J. Blinowska, R. Kus, and M. Kaminski, Phys. Rev. E **70**, 050902 (2004).

[7] D. W. Gow, J. A. Segawa, S. P. Ahlfors, and F. H. Lin, NeuroImage **43**, 614 (2008).

[8] N. Ancona, D. Marinazzo, and S. Stramaglia, Phys. Rev. E **70**, 056221 (2004).

[9] D. Marinazzo, M. Pellicoro, and S. Stramaglia, Phys. Rev. E **73**, 066216 (2006).

[10] B. Gourevitch, R. L. Bouquin-Jeannes, and G. Faucon, Biol. Cybern. **95**, 349 (2006).

[11] A. Subasi, Comput. Biol. Med. **37**, 183 (2007).

[12] M. Z. Ding, S. L. Bressler, W. M. Yang, and H. L. Liang, Biol. Cybernet. **83**, 35 (2000).

[13] I. J. Leontaritis and S. A. Billings, Int. J. Syst. Sci. **18**, 189 (1987).

[14] I. J. Leontaritis and S. A. Billings, Int. J. Control **41**, 303 (1985).

[15] L. Ljung and I. Ieee, in *Imtc/2001: Proceedings of the 18th IEEE Instrumentation and Measurement Technology Conference, Vols. 1–3: Rediscovering Measurement in the Age of Informatics* (IEEE, New York, 2001).

[16] H. L. Wei, S. A. Billings, and J. Liu, Int. J. Control **77**, 86 (2004).

[17] S. Chen, X. X. Wang, and C. J. Harris, IEEE Trans. Contr. Syst. Tech. **16**, 78 (2008).

[18] M. Niedzwiecki, IEEE Trans. Autom. Control **33**, 955 (1988).

[19] S. Chen and S. A. Billings, Int. J. Control **49**, 1013 (1989).

[20] S. Chen, S. A. Billings, C. F. N. Cowan, and P. M. Grant, Int. J. Control **52**, 1327 (1990).

[21] C. Harris, X. Hong, and Q. Gan, *Adaptive Modelling, Estimation, and Fusion from Data: A Neurofuzzy Approach* (Springer-Verlag, Berlin, 2002).

[22] K. H. Chon, H. Zhao, R. Zou, and K. Ju, IEEE Trans. Biomed. Eng. **52**, 956 (2005).

[23] S. A. Billings and H. L. Wei, IEEE Trans. Neural Netw. **18**, 306 (2007).

[24] H. L. Wei and S. A. Billings, IEEE Trans. Pattern Anal. Machine Intell. **29**, 162 (2007).

[25] R. B. Pachori and P. Sircar, Signal Process. **88**, 415 (2008).

[26] Y. Li, H. L. Wei, and S. A. Billings, IEEE Trans. Contr. Syst. Technol. **19**, 656 (2011).

[27] L. A. Aguirre and S. A. Billings, Int. J. Bifurcation Chaos **4**, 109 (1994).

[28] L. A. Aguirre and S. A. Billings, Int. J. Bifurcation Chaos **5**, 449 (1995).

[29] S. A. Billings and H. L. Wei, Int. J. Syst. Sci. **36**, 137 (2005).

[30] Y. Li, H. L. Wei, S. A. Billings, and P. G. Sarrigiannis, J. Neurosci. Methods **196**, 151 (2011).

[31] H. L. Wei, S. A. Billings, and J. J. Liu, Int. J. Modell., Ident. Control **9**, 215 (2010).

[32] J. Rissanen, Automatica **14**, 465 (1978).

[33] A. Brovelli, M. Z. Ding, A. Ledberg, Y. H. Chen, R. Nakamura, and S. L. Bressler, Proc. Natl. Acad. Sci. (USA) **101**, 9849 (2004).

[34] M. Kaminski, M. Z. Ding, W. A. Truccolo, and S. L. Bressler, Biol. Cybern. **85**, 145 (2001).